

Published in final edited form as:

J Cell Physiol. 2007 December ; 213(3): 801–808. doi:10.1002/jcp.21153.

Patch-clamp ‘mapping’ of ion channel activity in human sperm reveals regionalisation and co-localisation into mixed clusters

MC Jiménez-González^{1,#}, Y Gu², J Kirkman-Brown⁴, CLR Barratt³, and S Publicover¹

¹School of Biosciences, University of Birmingham, Birmingham B15 2TT, UK

²Department of Physiology, The Medical School, University of Birmingham, Birmingham B15 2TT, UK

³Reproductive Biology and Genetics Research Group, West Wing The Medical School, University of Birmingham, Birmingham B15 2TT, UK

⁴Assisted Conception Unit, Birmingham Women’s Hospital, Birmingham B15 2TG, UK

Abstract

Ion channels are pivotal to many aspects of sperm physiology and function. We have used the patch clamp technique to investigate the distribution of ion channels in the plasma membrane of the head of human spermatozoa. We report that three types of activity are common in the equatorial and acrosomal regions of the sperm head. Two of these (a chloride-permeable anion channel showing long stable openings and a second channel which flickered between open and closed states and was dependent upon cytoplasmic factors for activity) were localised primarily to the equatorial segment. A third type, closely resembling the flickering activity but with different voltage sensitivity of P_{open} was more widely distributed but was not detectable over the anterior acrosome. In the anterior acrosomal area channels were present but showed very low levels of spontaneous activity. A unique feature of channel activity in the sperm equatorial region was co-localisation into mixed clusters, most patches were devoid of activity but ‘active’ patches typically contained 2 or more types of activity (in a single 200-300 nM diameter patch). We conclude that ion channels in the sperm membrane show regionalisation of type and activity and that the channels are clustered into functional groups, possibly interacting through local effects on membrane potential. (207)

Keywords

sperm; patch clamp; ion channel; clustering

Introduction

Ion channels are pivotal to many aspects of sperm physiology and function (Darzon et al, 1999; 2001) including motility (Ren et al, 2001; Quill et al, 2001; Gu et al, 2004), volume regulation (Yeung et al, 2002, 2003, 2004; Petruninka et al, 2004), pH sensitivity (Alavi and Cosson, 2005), hyperpolarisation of membrane potential during capacitation (Florman et al, 1998; Arnoult et al, 1999; Brewis et al, 2000; Munoz-Garay et al, 2001) and acrosome reaction (Breitbart and Spungin, 1997; Florman et al, 1998; Barratt and Publicover, 2001). As well as ligand/second messenger-regulated conductances, sperm express various voltage-

Corresponding author: S. Publicover School of Biosciences, University of Birmingham, Birmingham B15 2TT, UK
s.j.publicover@bham.ac.uk; Phone +44 121 414 5455 ; Fax +44 121 414 5925.

[#]Current address: School of Life and Health Sciences, Aston University, Aston Triangle, Birmingham B4 7ET

gated channels and ionotropic 'neuronal' transmitter receptors (Meizel, 2004). Sperm respond to stimuli and regulate their activities using both 2nd messenger and electrical signals. It has been suggested that sperm could be viewed as 'a neuron with a tail' (Meizel, 2004) though possibly 'swimming dendrite' might better reflect the minute size of a sperm. However, whereas a dendrite collects inputs and electrically integrates them (Gulledge et al, 2005), a sperm must distinguish between different stimuli and give discrete and appropriately timed responses (Publicover et al, 2007).

The mature spermatozoon is a small, specialised and highly polarised cell where distinct functions are localised to specific regions. Consequently, there is a necessary distinct compartmentalization for the separation of various signalling and metabolic pathways (Travis and Kopf, 2002). The distribution of ligand receptors and membrane ion channels reflects this compartmentalization (Darszon et al, 2006), allowing the sperm to generate spatially restricted, ligand-induced second messenger signals and specific responses (Darszon et al, 2006; Publicover et al, 2007). The internal structure of a mature sperm includes only a thin sliver of cytoplasm which surrounds the acrosomal vesicle and nucleus. The nucleus is highly condensed and dehydrated and contains relatively few pore complexes, which are restricted to the sperm neck region (Sutovsky et al, 1999). Thus passive spread of electrical signals from a point source at the sperm membrane is highly likely to be tightly limited, permitting localisation of electrical signalling.

Use of immunocytochemical techniques to investigate the distribution of receptors and ion channels in mammalian sperm has shown not only that they are localised to different parts of the cell (head, midpiece, tail) but often a 'punctate' pattern of staining, suggesting that receptors and channels are clumped rather than randomly distributed (Westenbroek and Babcock, 1999; Wennemuth et al, 2000; Trevino et al, 2001; Barfield et al, 2005; Darszon et al, 2006). It is quite likely that this reflects, at least in part, localisation of ion channels to membrane lipid 'rafts' (Martens et al, 2004). For instance, in cardiac muscle signal transduction molecules including L channels and K⁺ channels (Kv1.5) are localised to caveolae (O'Connell et al, 2004). Lipid rafts, including caveolin, are known to exist in mammalian sperm (Trevino et al, 2001; Cross, 2004; James et al, 2005; van Gestel et al, 2005; Selvaraj et al, 2006; Weerachathanukul et al, 2007). It is thus likely that the sperm membrane has signalling domains where receptors and downstream elements are clustered. In a cell using electrical signalling these could include voltage regulated and voltage regulating ion channels – an electrical signalling micro-domain.

The size and shape of the mature spermatozoon is such that standard electrophysiological techniques have proved extremely difficult to use. In particular, routine acquisition of patch clamp 'seals' on sperm has proved extremely difficult. Gorelik et. al (2002) recorded single channel activity in sea urchin sperm heads using the 'smart patch' (combined patch clamp-scanning ion-conductance microscopy) technique. More recently high success rates have been achieved in mammalian cells by patching the sperm head (human; Gu et al, 2004) and cytoplasmic droplet (mouse sperm; Kirichok et al, 2006). We reported previously that, using a low diameter patch pipette (≈ 300 nm diameter, typical resistance ≈ 75 M Ω), we can achieve stable patches with a success rate of 35% on the sperm head (Gu et al, 2004). Further improvement of this technique has permitted us, for the first time, to apply a direct approach (cell-attached patch) to investigating the distribution of functional ion channels on the membranes of human spermatozoa. Three channel types were found regularly on the head of human sperm. Analysis of their distribution showed (i) regionalisation – different channels were concentrated in different parts of the head and (ii) co-localisation – channels are clumped, multiple channel types occurring in a single patch far more frequently than expected for a random distribution.

Materials and Methods

Preparation and capacitation of spermatozoa

All donors were recruited at the Birmingham Women's Hospital (HFEA Centre #0119), in accordance with the Human Fertilisation and Embryology Authority Code of Practice. Approval was obtained from the Local Ethical Committee (#0472, #5570) and all donors gave informed consent. Semen was collected and motile cells selected by swim-up into sEBSS [NaCl (116.4 mM), KCl (5.4 mM), CaCl₂ (1.8 mM), MgCl₂ (1 mM), Glucose (5.5 mM), NaHCO₃ (25 mM), Na pyruvate (2.5 mM), Na lactate (19 mM), MgSO₄ (0.81 mM) and 0.3% BSA, pH 7.4] as described previously (Kirkman-Brown et al, 2000). Cells were then diluted to 6 million/ml and stored in sEBSS lacking BSA until use. For recording cells were allowed to settle on a coverslip previously coated with poly-D-lysine (0.01%) then incubated at 37°C (5% CO₂) for 30 min. The coverslip was then placed in a purpose-built recording chamber incorporating an agar bridge and Ag/AgCl reference electrode and patched as described below. Cells were selected for patching on the basis that they appeared morphologically normal and the head was firmly attached. Only cells in which the flagellum was beating were used for patching.

Electrophysiological recording

Electrodes were made from 1 mm (O.D.) filamented borosilicate electrode glass (GC100F; Clark Electromedical Instruments, Kent, UK). The pipette was mounted vertically and a Sutter MP-225 3-axis micropositioner was used to lower the pipette axially onto the cell surface, as described previously (Fig 1a-c). A gently tapering electrode shank permitted visualization of the electrode tip and a magnified video image was used to achieve correct positioning (Gu et al, 2004). We achieved gigaseals in >55% of attempts. Holding potential was always 0 mV. All patching was carried out at room temperature (20-22 °C). Temperature did not vary by more than 0.5 °C during any experimental session.

Solution and chemicals

Extracellular and pipette saline was EBSS (Sigma; including [mM] 1.8 Ca²⁺, 117.5 Na⁺, 5.4 K⁺) except where stated otherwise. Pipettes filled with EBSS typically had resistance of 96-110 MΩ. Recordings were made using BioLogic RK-400 amplifier with low pass filter at 2 kHz. Generation of experimental protocols, data acquisition and analysis were carried out using pClamp 9.0. Signals were digitised at 10 kHz.

Statistical analysis

Analysis of the distribution of channel activity between sperm membrane compartments (anterior acrosomal and equatorial) was carried out by using chi square contingency tables. 'Clumping' of channels (non-random co-localisation within a patch) was analysed by calculating the probability that the observed co-localisation of channel activity could occur randomly. This was done by calculating the probabilities of occurrence of flickering (types 1 and 2) and long opening (type 3) channels in any patch and applying the bi-nomial distribution to determine the probability that the observed frequency of co-localisation could occur at random.

Results

Channel activity in cell-attached patches from the head of human sperm

From 454 attempts we obtained 247 good (>5 gigohm) seals on the heads of human sperm (≈55% success rate). Obtaining seals in the post acrosomal region proved extremely difficult (possibly due to the shape of the head) so >95% of records were obtained from the

equatorial and anterior acrosomal regions (fig 2). We detected active channels in 49/249 patches ($\approx 20\%$). Incidence of channel activity did not appear to vary between donors. In 21 of the 49 patches in which channels were present activity was virtually continuous (figs 3-5). Duration of recording ranged from 2-40 min (according to stability of the seal) allowing assessment of channel conductance, voltage dependence of open probability and distribution of open and closed times. Three types of channel activity were repeatedly observed. Two of these (referred to as type 1 and type 2) were superficially similar, showing flickering between the open and closed state with periodic longer openings (fig 3). Currents through these channels reversed at a value of membrane potential approximately 55 mV positive to resting potential. Type 1 showed some rectification, single channel conductance being approximately 28 pS at voltages negative to resting potential but increasing with depolarisation. Open probability was highest at resting potential plus 18 mV ($n=13$; fig 3). Type 2 activity also flickered between open and closed states, but had a lower conductance (23 pS) and showed maximum open probability at a holding potential 15 mV negative to resting potential ($n=7$; fig 3), more than 30 mV more negative than that in type 1 activity (compare lower panels in fig 3). A third type of channel was seen (type 3) with a conductance of 31 pS. The kinetics of this channel were very different, with prolonged, more stable openings, particularly at depolarised potentials (fig 4a,b). Reversal potential was estimated to be 70-75 mV positive to resting potential ($n=9$; fig 4c).

In addition, we observed activity in another 28 patches (fig 2; yellow). In these the activity was much more variable and occurred only periodically. In every case the channel flickered between open and closed states, but current amplitudes were often very different to those in type 1 or type 2 channels and activity appeared only occasionally in a series of voltage steps. Current amplitude was usually stable within bursts of activity (fig 4d) but attempts to create a current-voltage plot in order to determine conductance generated a scatter rather than a line or curve (fig. 4e). Activity was sufficiently rare that simultaneous openings were not observed. However, switching between sub-conductance states was never seen, suggesting that these patches contained more than one channel (see below).

Clustering of channels in sperm

During collection of these data it became clear that the channels showed regionalisation in their distribution (fig 5). Whereas type 1 was distributed randomly between the anterior acrosomal and equatorial regions (Fig 2 green; $P>0.5$; chi square), type 2 was seen only in the equatorial region and type 3 occurred there in 8 of the 9 patches in which its activity was detected ($P<0.005$; chi square). Furthermore, in the equatorial area, where activities of all three of the continuously active conductances were detected, the channels were spatially associated. Of 10 patches in the equatorial region in which tonic channel activity was observed, eight clearly had more than one channel type within the patch (fig 2 red; table 1). Type 2 and 3 activities were never observed in isolation and in 7 of the 'multi-conductance' patches all three activities were present (table 1). Within these patches individual channels showed periods of increased activity such that it was occasionally possible to obtain data, from a complete command protocol, for just one channel type. The traces shown in figs 3 and 4a (showing channel types 1, 2 and 3) were all obtained from the same cell-attached patch. Coincident activity was also observed. Fig 6a shows more records from the same patch in which opening of two channels, or a large channel with a sub-conductance state, apparently occurs. Conductances indicate that two channels of type 1 and/or type 2 are probably responsible (also observed independently in this patch; fig 2), but the open state is more stable than when gating independently and opening of the two channels is often synchronised.

To establish simply that co-localisation of channel types in the equatorial region was real (not random) we categorised all flickering channel activity (type 1 or 2) as type 'F' and the

activity of type 3 (long openings) as type 'L'. In the equatorial region the probability of observing activity F in any patch was 0.098 (10/102). For activity L the probability was 0.079 (8/102). If the activities were randomly distributed, the likelihood of observing both in any patch is 0.008 (0.098×0.079). From the binomial distribution, the probability that F and L activity would be co-incident in 8 or more out of 102 patches (as was observed) is <0.00001 .

Channel selectivity and permeability

Since intracellular ion concentrations in sperm are largely unknown, reversal potential in cell-attached mode provides very limited information about channel ion selectivity. We therefore attempted to use the inside-out configuration, allowing variation of the saline bathing the inner face of the patch. Though this configuration proved very difficult to obtain by the usual approach of pulling the pipette away from the cell, we did on a number of occasions find that this configuration occurred spontaneously after achieving cell-attached patch. Surprisingly, under these conditions only the type 3 (long openings) channel was observed, with a conductance of 33 pS. Reversal (as expected in symmetric conditions) was close to zero and the currents were slightly outwardly rectified (fig 6b). When we perfused the bath with sEBSS made with Na gluconate (substituted for NaCl, a reduction of $[Cl^-]_o$ from 129 mM to 39 mM), the conductance of the channels was slightly decreased (29 pS; $n=3$) and the reversal potential was shifted by +24 mV ($n=3$). The change in the calculated E_{Cl} due to Cl^- substitution is +30.0 mV. Thus this is a chloride permeable anion channel but not Cl^- selective.

Discussion

Despite their great importance, the nature and distribution of ion channels in sperm are largely unknown. Data from immuno-cytochemical studies strongly suggest that ion channel proteins are not randomly distributed in the sperm membrane, but only direct electrophysiological recording can permit assessment of the distribution of channel activity. Using the technique for patching human sperm that we described previously (Gu et al, 2004), we obtained gigaseals on the head of human sperm in over 55% of attempts. It seems likely that the shape of the human sperm head is better suited to formation of cell-attached patches than that of mouse sperm, where seal formation has proved particularly difficult (Kirichok et al, 2006). This high rate of seal formation has allowed us to 'map' the distribution of channel activity over the equatorial and anterior acrosomal areas of human sperm. Though more than 80% of patches were 'silent' three types of channel activity were commonly observed, all showing reversal positive to resting potential. One of these had a conductance of approximately 31 pS in cell attached recordings and in inside out recording was shown to be a Cl^- -permeable anion channel. Espinosa et al (1998) observed anion channels in patches on the head of mouse sperm. Under the conditions used (pipette saline containing 129 mM chloride) the channel showed three conductance states one of which was 30 pS. This channel was sensitive to niflumic acid, which also inhibited acrosome reaction at similar doses (Espinosa et al., 1998). Chloride channels have been implicated in regulation of acrosome reaction in human sperm (Meizel, 1997) and future work must address the possible significance of the 31 pS chloride-permeable channel in this process. The other two commonly observed activities had similar conductances (23/28 pS) and flickering activities. Voltage dependence of P_{open} , however, differed markedly between the two types, indicating either that these were different channels types or the same channel type in different states, possibly related to regulation by 2nd messengers. Intriguingly, both these activities were lost when the pipette was pulled off the membrane to achieve inside out configuration, suggesting that a cytoplasmic factor is essential to maintain activity. It was not possible to investigate selectivity in inside-out patches but some assessment can be made

on the basis that reversal potential of these channels in cell-attached mode was approximately 55 mV positive to resting potential giving a probable E_{rev} of 0 to +10 mV. Estimates of intracellular concentrations of the major ions have been made in populations of mammalian sperm. For a $[K^+]_i$ of 90-120 mM (Babcock, 1983; Zeng et al, 1995) E_K is between -71 and -78 mV. $[Na^+]_i$ is estimated at 14 to 17.8 mM (Babcock, 1983; Patrat et al, 2000) giving E_{Na} of +55 to +62 mV. $[Cl^-]_i$ is estimated at up to 69 mM (though this may be a conservative estimate; Garcia and Meizel, 1999) giving an E_{Cl} of -15 mV. Thus reversal for the channel is closest to E_{Cl} but it is likely that the channels are not Cl^- -selective and these could even be a non-selective channels. Supplementation of media to prevent rundown in inside-out mode will permit more thorough investigation.

The distribution of these channels on the sperm head was clearly structured. The type 1 activity was widely distributed but did not occur at the apex of the acrosomal region. The Cl^- permeable channel (type 3) and the type 2 activity were observed primarily in the equatorial region of the cells (8 out of 9 patches for each), though the distribution of these channels may have extended further back. Intermittent activity that apparently reflected activity of other channels (yellow dots in fig 1b) was virtually absent from the equatorial region but was common over the acrosome.

Activity of these channels was very rare and it was impossible to obtain I-V plots. The plasmalemma of the sperm can be divided into anterior acrosomal, equatorial and post acrosomal regions (Primakoff et al, 1983; James et al, 2005). The anterior acrosome (and possibly the equatorial region) interacts with the extracellular matrix of the egg and the equatorial segment (in acrosome reacted cells) fuses with the oolemma (Bedford et al, 1979). Recent data suggest that the membrane of the sperm head is structured, with different characteristics in these two areas (James et al, 2005; van Gestel et al, 2005; Selveraj et al, 2006). The distribution of channel activity reported here complements these observations, showing that sperm are both structurally and physiologically regionalised. If activity types 1 and 2 do reflect regulation of the same channel then this regulation is localised.

Even more strikingly, the channels were tightly grouped. 75% of patches showed no detectable channel activity, yet in those patches where activity was sufficient for analysis almost half contained two, three or more conductances. We (Gu et al, 2004) and others (Beltran et al, 1994; Espinosa et al, 1998) have previously reported the presence of channels with multiple sub-conductance states in sperm of humans and other mammals. Occasionally closing of the different components of activity in multi-conductance patches was simultaneous, consistent with interpretation as sub-conductance states of a single channel. However, even in these patches we regularly saw discrete activity of individual conductance components, which themselves displayed sub-conductances states (fig 5a). We conclude that the different conductances reflect the co-localisation, within a single patch, of several channels. Furthermore, in those patches where activity was rare and apparently variable in character (fig 4c,d) it is likely that more than 1 channel was co-localised. The diameter of our patch pipettes was only 0.2-0.3 μm (measured by scanning electron microscopy; pipette resistance was consistently 90-100 M Ω), thus these channels are extremely closely associated. This finding is potentially of great significance in understanding the physiology of these cells. Sperm are rich in voltage-dependent membrane channels (Darszon et al, 1999) and electrophysiological mechanisms (regulation of ion channels by membrane voltage and/or ionotropic signals) are pivotal to their functioning. Achieving discrete and accurate control of electrically regulated activities in this minute cell thus demands the existence of sub-cellular electrophysiological events and the existence of discrete membrane potential domains. Loss of cytoplasm, nuclear condensation and restriction of nuclear pores to the neck region of the sperm (Sutovsky et al, 1999) during spermiogenesis will 'pre-adapt' sperm for this purpose. Since passive spread of voltage through the cytoplasm will be very

limited (see introduction), activity of membrane ion channels will cause localised voltage transients affecting only neighbouring channels - those within a cluster. Thus clustering of channels in closely associated groups, as reported here is likely to be pivotal to rapid electrical signalling. Application of scanning ion-conductance microscopy, using ultra-fine quartz pipettes (Shevchuk et al. 2006) may provide an ideal independent method for corroborating and quantifying this clustering

In summary, application of patch clamp to the heads of human sperm reveals a remarkable level of physiological localisation. Different parts of the sperm possess different channels and in areas with multiple channel types there is a remarkable clustering which is almost certainly functionally significant. An important future goal is to assess the ability of sperm to generate localised electrical signals, thus permitting 'instant' but spatially discrete responses.

Acknowledgments

This work was supported by the Wellcome Trust (Grant # 069093)

References

- Alavi SM, Cosson J. Sperm motility in fishes. I. Effects of temperature and pH: a review. *Cell Biol Int*. 2005; 29:101–110. [PubMed: 15774306]
- Arnoult C, Kazam IG, Visconti PE, Kopf GS, Villaz M, Florman HM. Control of the low voltage-activated calcium channel of mouse sperm by egg ZP3 and by membrane hyperpolarization during capacitation. *Proc Natl Acad Sci U S A*. 1999; 96:6757–6762. [PubMed: 10359785]
- Barfield JP, Yeung CH, Cooper TG. Characterization of potassium channels involved in volume regulation of human spermatozoa. *Mol Hum Reprod*. 2005; 11:891–897. [PubMed: 16421215]
- Barratt CL, Publicover SJ. Interaction between sperm and zona pellucida in male fertility. *Lancet*. 2001; 358:1660–1662. [PubMed: 11728536]
- Bedford JM, Moore HD, Franklin LE. Significance of the equatorial segment of the acrosome of the spermatozoon in eutherian mammals. *Exp Cell Res*. 1979; 119:119–126. [PubMed: 581665]
- Beltran C, Darszon A, Labarca P, Lievano A. A high-conductance voltage-dependent multistate Ca^{2+} channel found in sea urchin and mouse spermatozoa. *FEBS Lett*. 1994; 338:23–26. [PubMed: 8307151]
- Breitbart H, Spungin B. The biochemistry of the acrosome reaction. *Mol Hum Reprod*. 1997; 3:195–202. [PubMed: 9237245]
- Brewis IA, Morton IE, Mohammad SN, Browes CE, Moore HD. Measurement of intracellular calcium concentration and plasma membrane potential in human spermatozoa using flow cytometry. *J Androl*. 2000; 21:238–249. [PubMed: 10714818]
- Cross NL. Reorganization of lipid rafts during capacitation of human sperm. *Biol Reprod*. 2004; 71:1367–1373. [PubMed: 15215196]
- Darszon A, Acevedo JJ, Galindo BE, Hernandez-Gonzalez EO, Nishigaki T, Trevino CL, Wood C, Beltran C. Sperm channel diversity and functional multiplicity. *Reproduction*. 2006; 131:977–988. [PubMed: 16735537]
- Darszon A, Beltran C, Felix R, Nishigaki T, Trevino CL. Ion transport in sperm signaling. *Dev Biol*. 2001; 240:1–14. [PubMed: 11784043]
- Darszon A, Labarca P, Nishigaki T, Espinosa F. Ion channels in sperm physiology. *Physiol Rev*. 1999; 79:481–510. [PubMed: 10221988]
- Espinosa F, de la Vega-Beltran JL, Lopez-Gonzalez I, Delgado R, Labarca P, Darszon A. Mouse sperm patch-clamp recordings reveal single Cl^- channels sensitive to niflumic acid, a blocker of the sperm acrosome reaction. *FEBS Lett*. 1998; 426:47–51. [PubMed: 9598976]
- Florman HM, Arnoult C, Kazam IG, Li C, O'Toole CM. A perspective on the control of mammalian fertilization by egg-activated ion channels in sperm: a tale of two channels. *Biol Reprod*. 1998; 59:12–16. [PubMed: 9674987]

- Gorelik J, Gu Y, Spohr HA, Shevchuk AI, Lab MJ, Harding SE, Edwards CR, Whitaker M, Moss GW, Benton DC, Sanchez D, Darszon A, Vodyanoy I, Klenerman D, Korchev YE. Ion channels in small cells and subcellular structures can be studied with a smart patch-clamp system. *Biophys J*. 2002; 83:3296–3303. [PubMed: 12496097]
- Gu Y, Kirkman-Brown JC, Korchev Y, Barratt CL, Publicover SJ. Multistate, 4-aminopyridine-sensitive ion channels in human spermatozoa. *Dev Biol*. 2004; 274:308–317. [PubMed: 15385161]
- Gulledge AT, Kampa BM, Stuart GJ. Synaptic integration in dendritic trees. *J Neurobiol*. 2005; 64:75–90. [PubMed: 15884003]
- James PS, Hennessy C, Berge T, Jones R. Compartmentalisation of the sperm plasma membrane: a FRAP, FLIP and SPFI analysis of putative diffusion barriers on the sperm head. *J Cell Sci*. 2005; 117:6485–6495. [PubMed: 15572407]
- Kirichok Y, Navarro B, Clapham DE. Whole-cell patch-clamp measurements of spermatozoa reveal an alkaline-activated Ca^{2+} channel. *Nature*. 2006; 439:737–740. [PubMed: 16467839]
- Kirkman-Brown JC, Bray C, Stewart PM, Barratt CL, Publicover SJ. Biphasic elevation of $[\text{Ca}^{2+}]_i$ in individual human spermatozoa exposed to progesterone. *Dev Biol*. 2000; 222:326–335. [PubMed: 10837122]
- Martens JR, O'Connell K, Tamkun M. Targeting of ion channels to membrane microdomains: localization of K_v channels to lipid rafts. *Trends Pharmacol Sci*. 2004; 25:16–21. [PubMed: 14723974]
- Meizel S. Amino acid neurotransmitter receptor/chloride channels of mammalian sperm and the acrosome reaction. *Biol Reprod*. 1997; 56:569–574. [PubMed: 9046998]
- Meizel S. The sperm, a neuron with a tail: 'neuronal' receptors in mammalian sperm. *Biol Rev Camb Philos Soc*. 2004; 79:713–732. [PubMed: 15682867]
- Munoz-Garay C, De la Vega-Beltran JL, Delgado R, Labarca P, Felix R, Darszon A. Inwardly rectifying K^+ channels in spermatogenic cells: functional expression and implication in sperm capacitation. *Dev Biol*. 2001; 234:261–274. [PubMed: 11356034]
- O'Connell KM, Martens JR, Tamkun MM. Localization of ion channels to lipid Raft domains within the cardiovascular system. *Trends Cardiovasc Med*. 2004; 14:37–42. [PubMed: 15030787]
- Petrunkina AM, Harrison RA, Ekhlas-Hundrieser M, Topfer-Petersen E. Role of volume-stimulated osmolyte and anion channels in volume regulation by mammalian sperm. *Mol Hum Reprod*. 2004; 10:815–823. [PubMed: 15361553]
- Primakoff P, Myles DG. A map of the guinea pig sperm surface constructed with monoclonal antibodies. *Dev Biol*. 1983; 98:417–428. [PubMed: 6683688]
- Publicover SJ, Harper CV, Barratt CL. $[\text{Ca}^{2+}]_i$ signalling in sperm – making the most of what you've got. *Nature Cell Biol*. 2007 (in press).
- Quill TA, Ren D, Clapham DE, Garbers DL. A voltage-gated ion channel expressed specifically in spermatozoa. *Proc Natl Acad Sci U S A*. 2001; 98:12527–12531. [PubMed: 11675491]
- Ren D, Navarro B, Perez G, Jackson AC, Hsu S, Shi Q, Tilly JL, Clapham DE. A sperm ion channel required for sperm motility and male fertility. *Nature*. 2001; 413:603–609. [PubMed: 11595941]
- Shevchuk AI, Frolenkov GI, Sanchez D, James PS, Freedman N, Lab MJ, Jones R, Klenerman D, Korchev YE. Imaging proteins in membranes of living cells by high-resolution scanning ion conductance microscopy. *Angew Chem Int Ed Engl*. 2006; 45:2212–2216. [PubMed: 16506257]
- Selvaraj V, Asano A, Buttke DE, McElwee JL, Nelson JL, Wolff CA, Merdiushev T, Fornes MW, Cohen AW, Lisanti MP, Rothblat GH, Kopf GS, Travis AJ. Segregation of micron-scale membrane sub-domains in live murine sperm. *J Cell Physiol*. 2006; 206:636–646. [PubMed: 16222699]
- Sutovsky P, Ramalho-Santos J, Moreno RD, Oko R, Hewitson L, Schatten G. On-stage selection of single round spermatids using a vital, mitochondrion-specific fluorescent probe MitoTracker(TM) and high resolution differential interference contrast microscopy. *Hum Reprod*. 1999; 14:2301–2312. [PubMed: 10469700]
- Travis AJ, Kopf GS. The role of cholesterol efflux in regulating the fertilization potential of mammalian spermatozoa. *J Clin Invest*. 2002; 110:731–736. [PubMed: 12235100]

- Trevino CL, Serrano CJ, Beltran C, Felix R, Darszon A. Identification of mouse trp homologs and lipid rafts from spermatogenic cells and sperm. *FEBS Lett.* 2001; 509:119–125. [PubMed: 11734218]
- Trevino CL, Serrano CJ, Beltran C, Felix R, Darszon A. Identification of mouse trp homologs and lipid rafts from spermatogenic cells and sperm. *FEBS Lett.* 2001; 509:119–125. [PubMed: 11734218]
- van Gestel RA, Brewis IA, Ashton PR, Helms JB, Brouwers JF, Gadella BM. Capacitation-dependent concentration of lipid rafts in the apical ridge head area of porcine sperm cells. *Mol Hum Reprod.* 2005; 11:583–590. [PubMed: 16051681]
- Weerachatanukul W, Proboadh I, Kongmanas K, Tanphaichitr N, Johnston LJ. Visualizing the localization of sulfoglycolipids in lipid raft domains in model membranes and sperm membrane extracts. *Biochim Biophys Acta.* 2007; 1768:299–310. [PubMed: 17045957]
- Wennemuth G, Westenbroek RE, Xu T, Hille B, Babcock DF. $\text{Ca}_v2.2$ and $\text{Ca}_v2.3$ (N- and R-type) Ca^{2+} channels in depolarization-evoked entry of Ca^{2+} into mouse sperm. *J Biol Chem.* 2000; 275:21210–21217. [PubMed: 10791962]
- Westenbroek RE, Babcock DF. Discrete regional distributions suggest diverse functional roles of calcium channel $\alpha 1$ subunits in sperm. *Dev Biol.* 1999; 207:457–469. [PubMed: 10068476]
- Yeung CH, Anapolski M, Sipila P, Wagenfeld A, Poutanen M, Huhtaniemi I, Nieschlag E, Cooper TG. Sperm volume regulation: maturational changes in fertile and infertile transgenic mice and association with kinematics and tail angulation. *Biol Reprod.* 2002; 67:269–275. [PubMed: 12080027]
- Yeung CH, Barfield JP, Anapolski M, Cooper TG. Volume regulation of mature and immature spermatozoa in a primate model, and possible ion channels involved. *Hum Reprod.* 2004; 19:2587–2593. [PubMed: 15319384]
- Yeung CH, Anapolski M, Depenbusch M, Zitzmann M, Cooper TG. Human sperm volume regulation. Response to physiological changes in osmolality, channel blockers and potential sperm osmolytes. *Hum Reprod.* 2003; 18:1029–1036. [PubMed: 12721181]

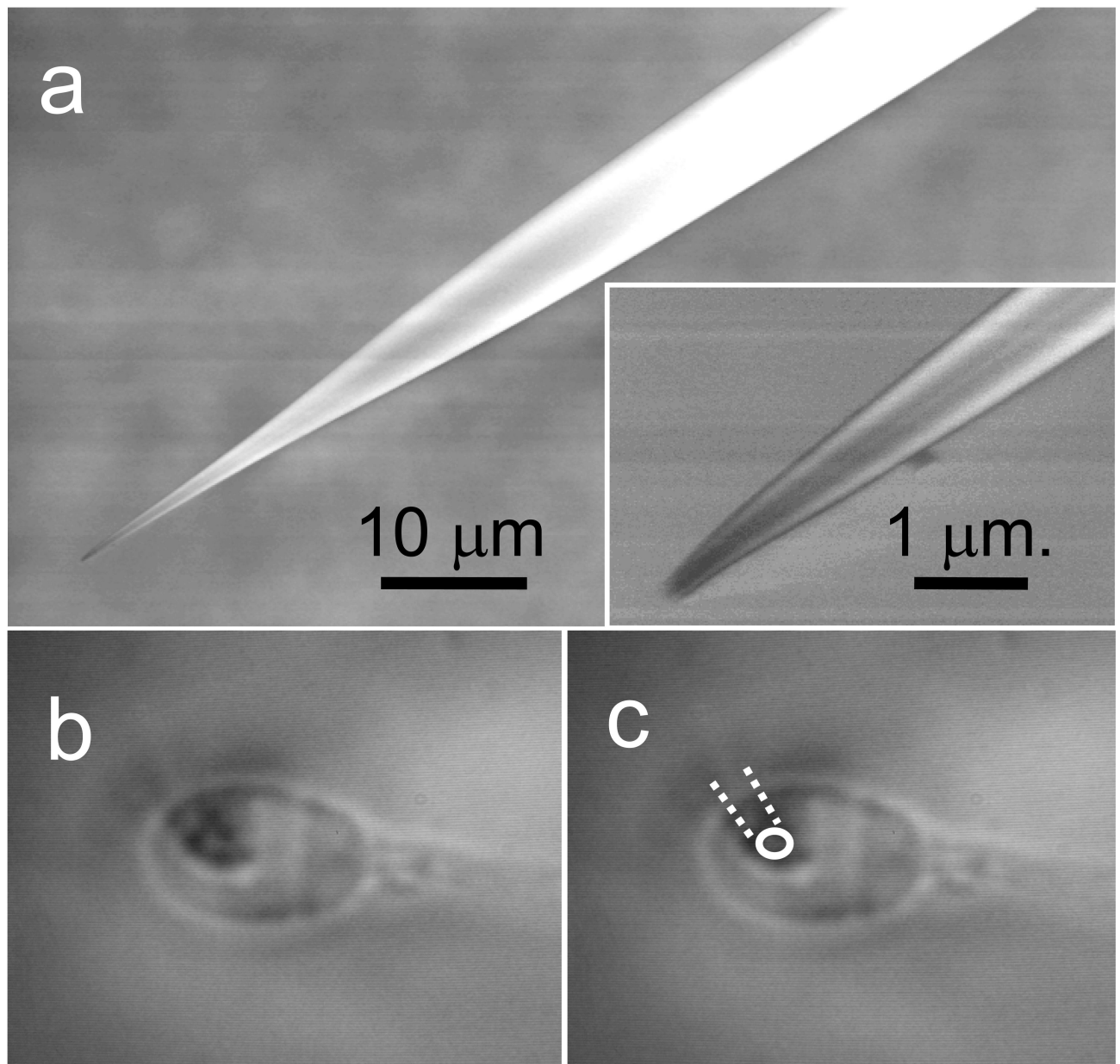


Fig 1. Obtaining patches on the head of human spermatozoa. (a) Scanning electron micrograph of the fine patch pipettes used in this study. The final 20 μm of the pipette tapers gently to a tip of ≈300 nm (see inset), (b) Example of video image used during approach to the cell surface. Picture shows a sperm head with the tip of the pipette visible as a ring. The diameter is exaggerated due to light diffraction around the tip but the centre can be clearly located. In this instance the pipette is slightly off vertical and the shank is just visible (highlighted in 'c').

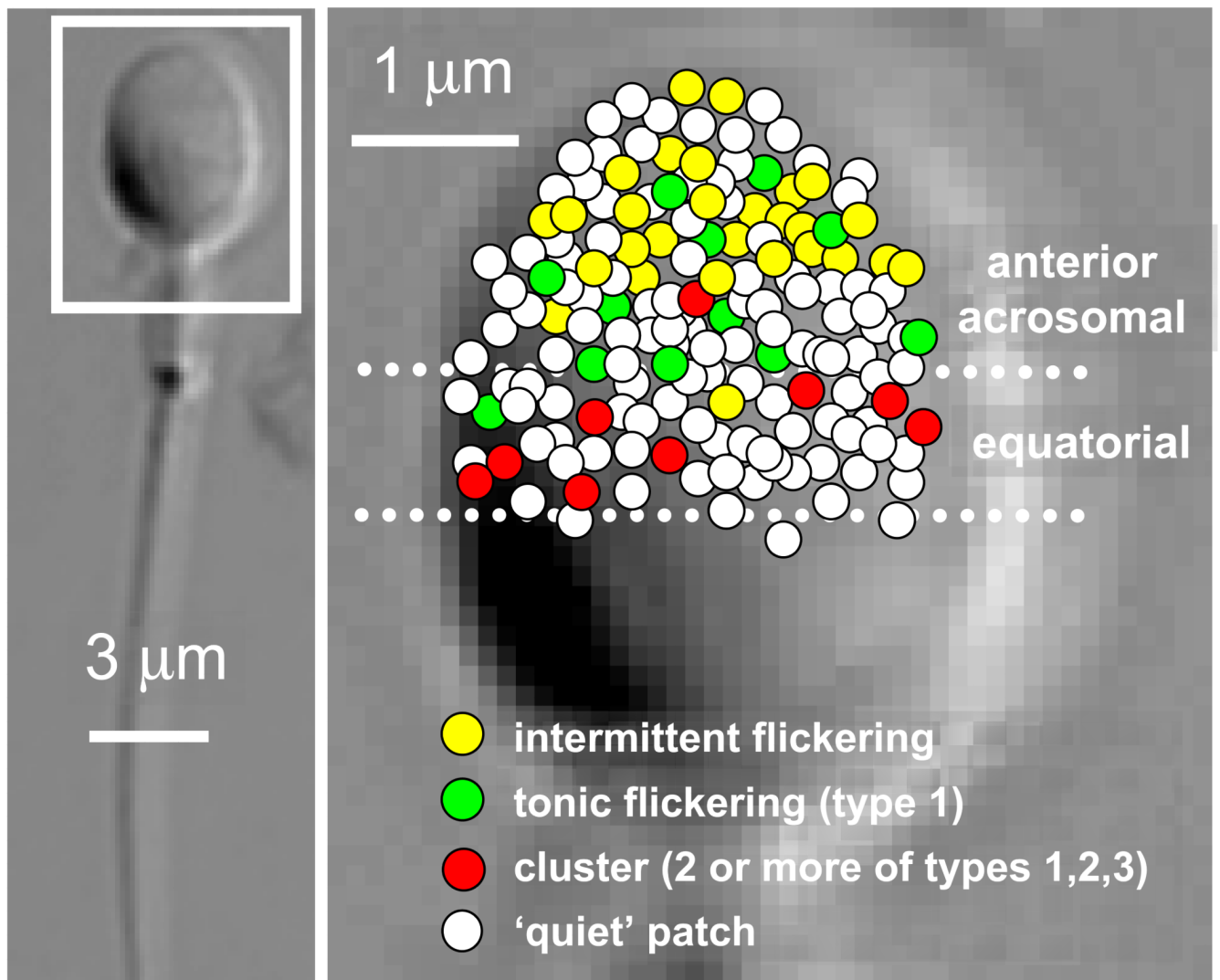


Fig. 2. Mapping of ion channel distribution on the head of human sperm. The position of each patch was recorded using the image as shown in fig 1c and combined to produce the composite image. All patches shown are in the equatorial and acrosomal areas. Colours show patches containing channel type 1 (green); mixed clusters of at least two of types 1, 2 and 3 (red) or intermittent flickering activity (yellow). White circles are 'quiet' patches. Dashed lines show boundaries used to allocate patches to anterior-acrosomal and equatorial areas.

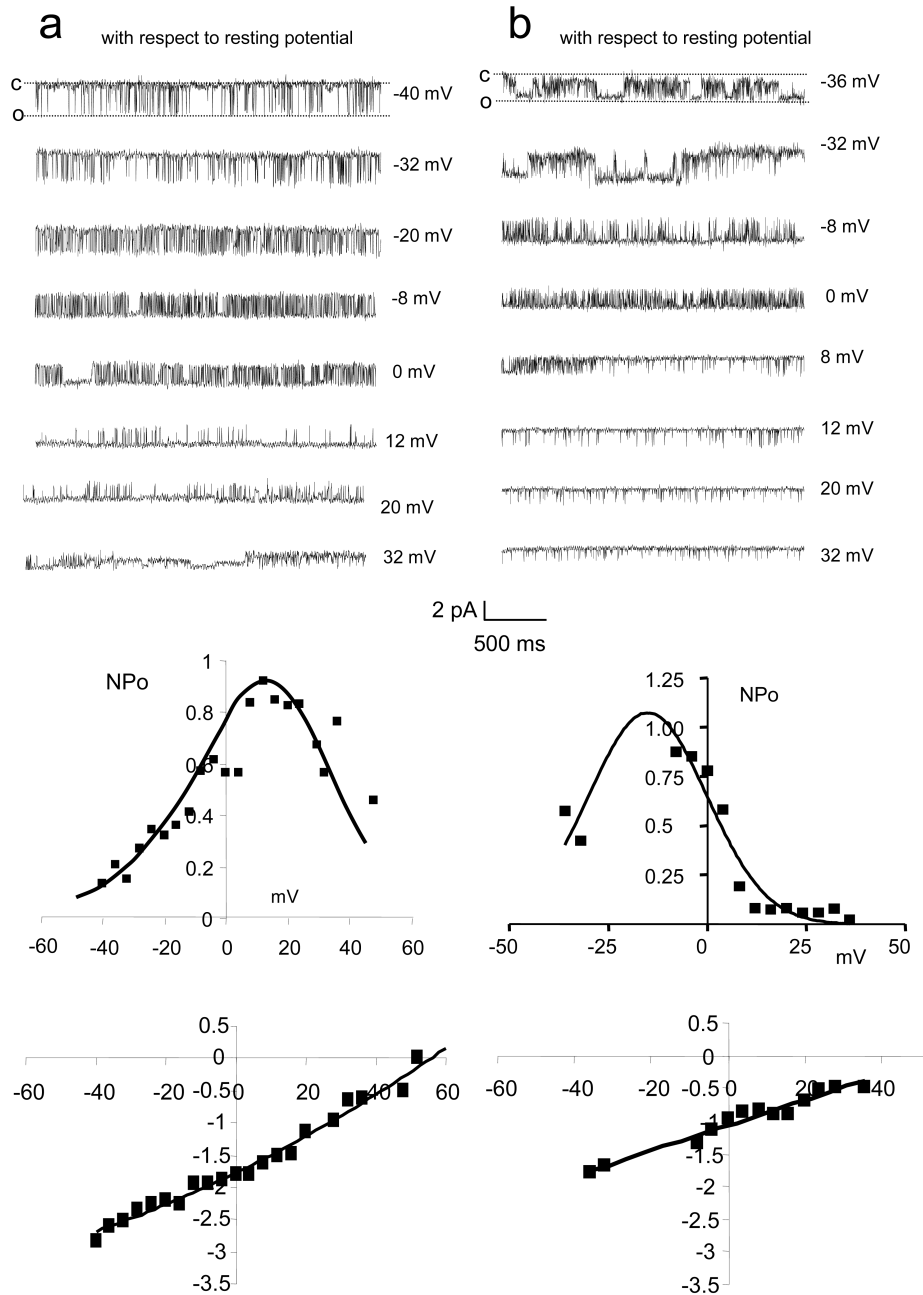


Fig. 3. Characteristics of activity type 1 (a: patches shown green and in red in fig 2) and type 2 (b: most red patches in fig 2). (a) upper panel - representative traces from a type 1 channel at a series of patch potentials from -40 mV (with respect to resting potential) to 32 mV positive to resting potential. Downward transitions are opening (inward current). Channel shows constant flickering activity at all potentials. Centre panel - open probability (NPo) of type I activity is voltage dependent and is highest at 20 - 30 mV positive to resting potential. Lower panel - current-voltage plot for single type 1 channel currents. Gradient gives a conductance of ≈ 28 pS and the current reverses at \approx resting potential $+55$ mV. (b) Upper panel - representative traces from a type 2 channel at a series of patch potentials from

potentials from -36 mV (with respect to membrane potential) to 32 mV positive to resting potential. Downward transitions are opening (inward current). Channel shows constant flickering activity at all potentials. Centre panel - open probability (NPo) of type 2 activity is voltage dependent and is highest at 10 - 20 mV negative to resting potential. Lower panel - current-voltage plot for single type 2 channel currents. Gradient gives a conductance of ≈ 23 pS and the current reverses at \approx resting potential $+55$ mV.

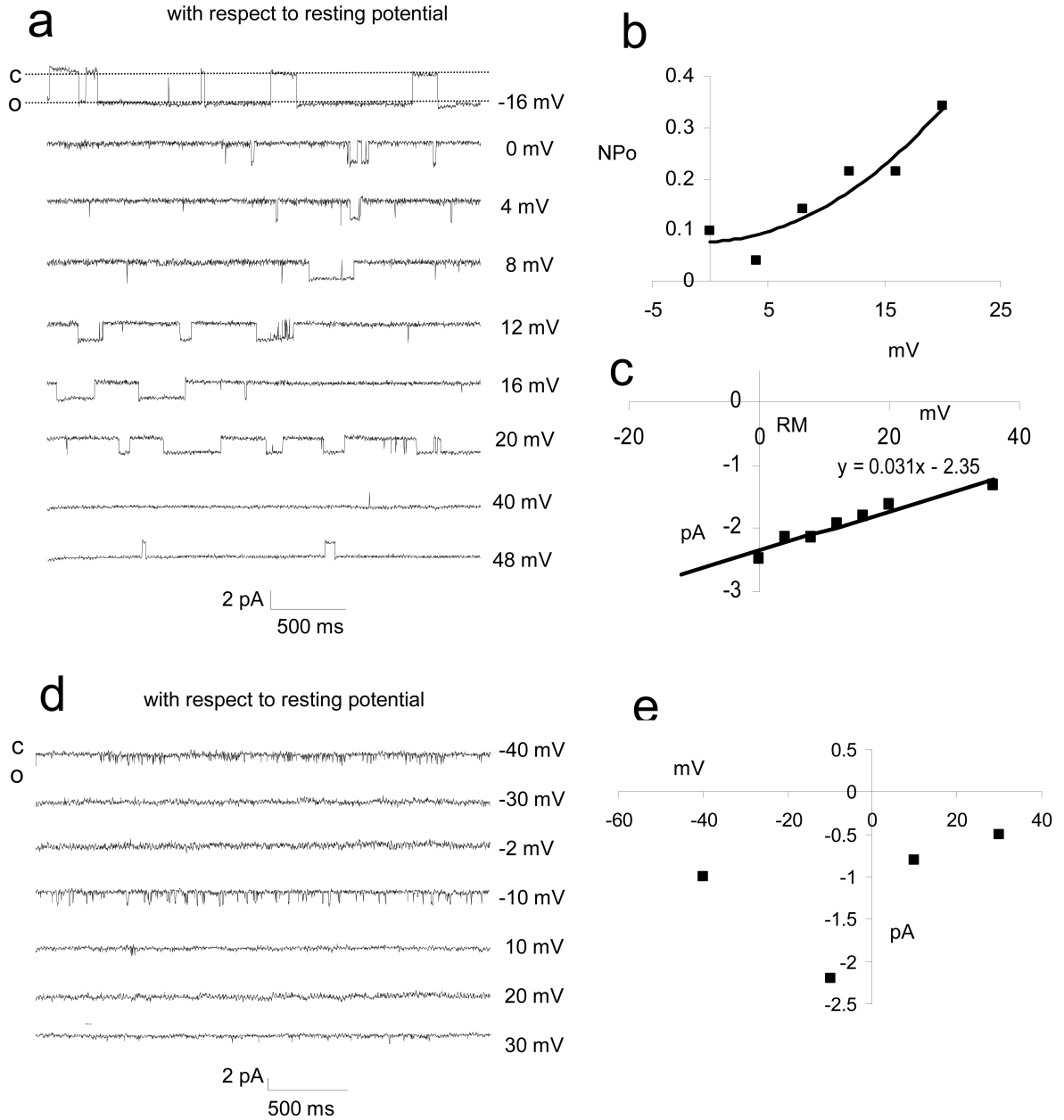


Figure 4. Characteristics of channel type 3 (a-c; patches shown red in fig 2) and intermittent/variable ‘flickering’ activity (d-e: yellow patches in fig 2).. (a) representative traces from a channels at a series of pipette potentials from potentials from -16 mV (with respect to membrane potential) to 48 mV positive to resting potential. Downward transitions are opening (inward current). Channel shows constant flickering activity at all potentials. (b) Open probability (NPo) is voltage dependent and increases at potentials positive to resting potential. (c) Current-voltage plot for single channel currents. Gradient gives a conductance of ≈ 31 pS and the current reverses at \approx resting potential $+75$ mV. (d) representative traces from one patch showing intermittent/variable ‘flickering’ activity. Records from -40 mV (with

respect to membrane potential) to 30 mV positive to resting potential. Downward transitions are opening (inward current). Activity was very rare and the four traces in which activity was discernible were not all collected during a single voltage-stepping protocol. (e) Current-voltage scattergram for the single channel currents from the patch with intermittent/variable 'flickering' activity shown in 'd'. The data cannot be fitted to a single conductance plot indicating that the patch contains more than one channel and/or channels have sub-conductance states.

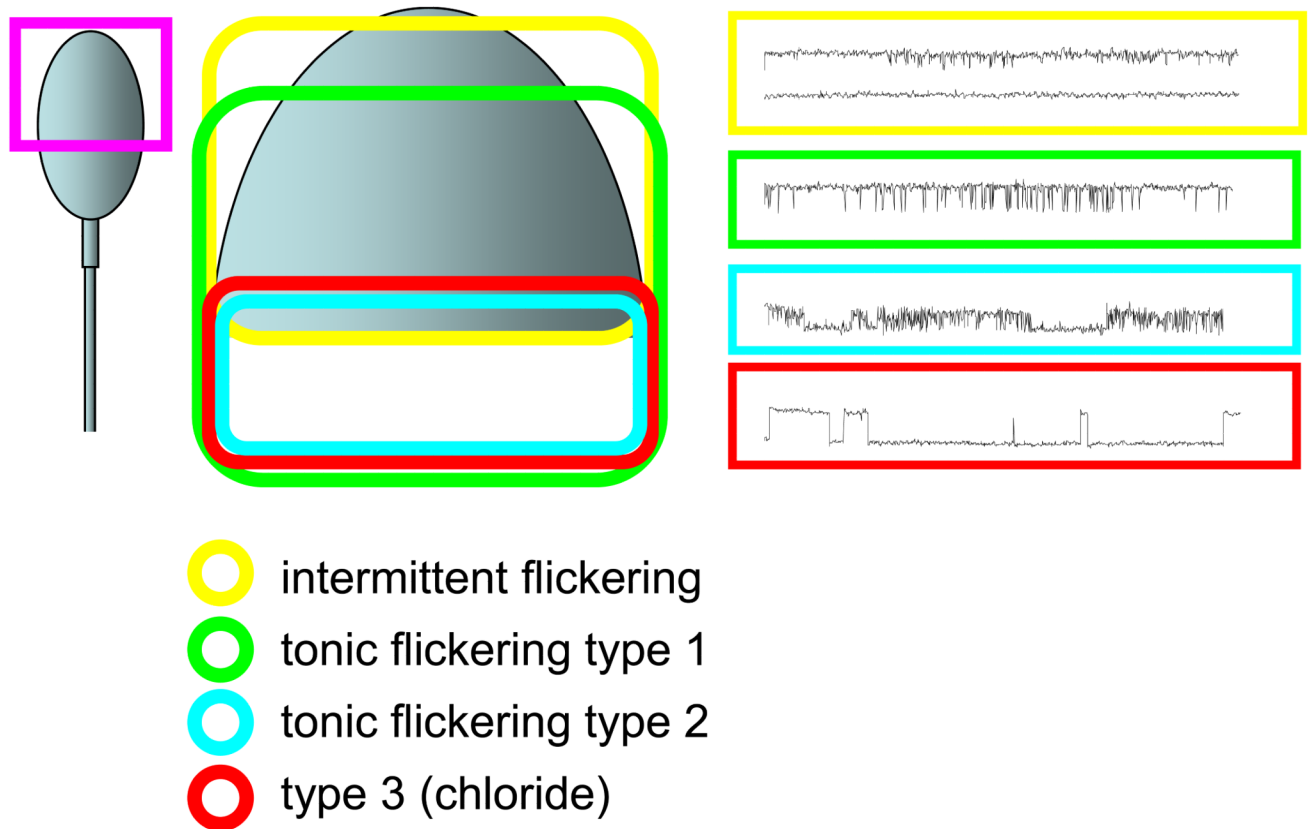


Figure 5. Schematic to show distribution of the four type of activity reported here. Intermittent flickering, tonic flickering type 1, tonic flickering type 2 and type 3 activity are shown by the yellow, green, blue and red contours respectively. Examples of ‘typical’ activity are shown to the right, using the same colour code.

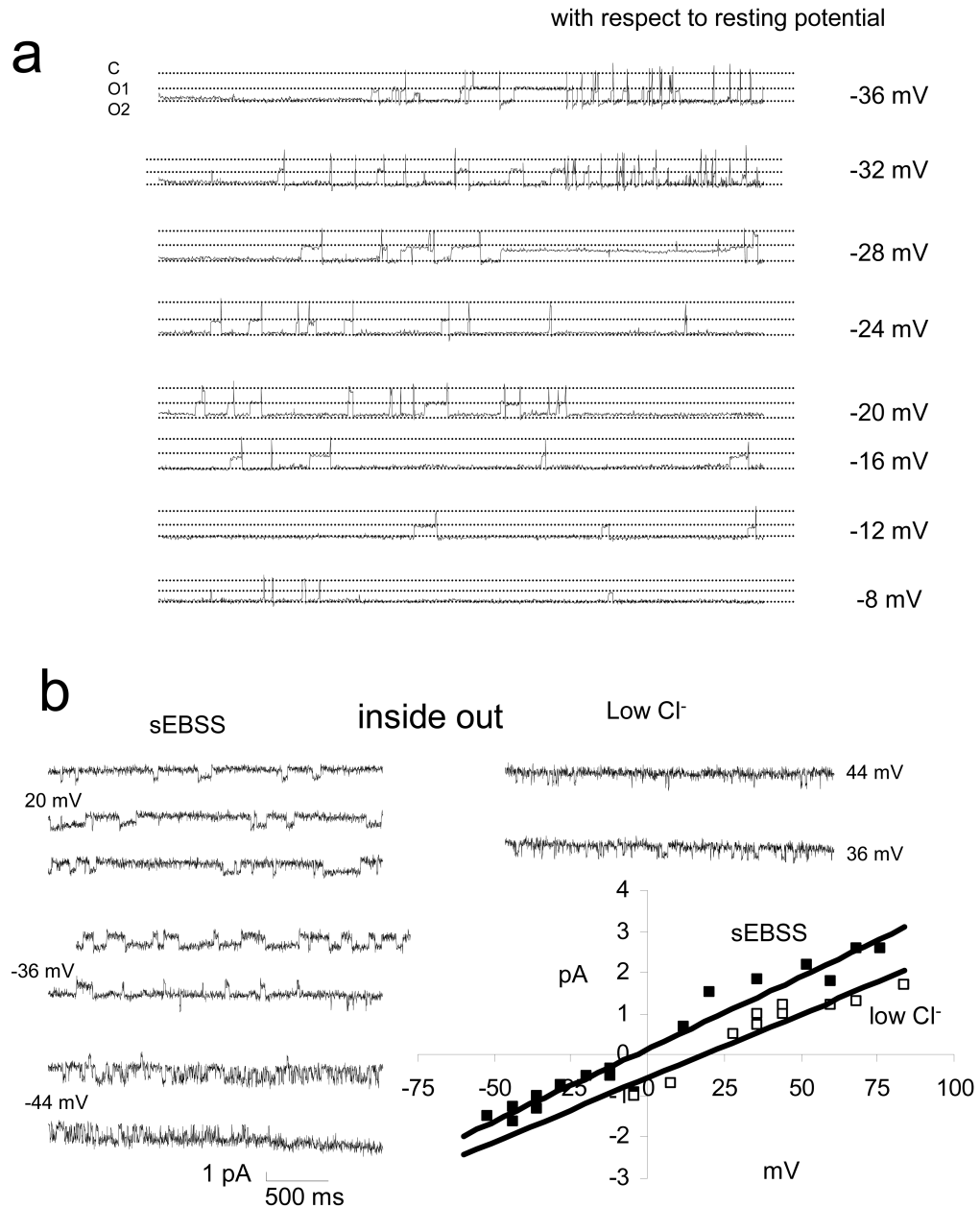


Figure 6.

Complex records and characterisation of type 3 channel. (a) Coincident activity of two channels with conductances of ≈ 25 pS (probably one each of type 1 and type 2, both of which were observed in this patch). Coincident activity shows more stable open states and opening is usually synchronous. (b) Modulation of current through type 3 channel by substitution of Cl⁻ with gluconate. Left panel shows currents recorded at 3 different pipette potentials in an inside-out patch (symmetrical conditions). Upper right panel shows currents recorded after replacement of sEBSS ([Cl⁻] = 129 mM) in the bath (cytoplasmic face of patch) with modified saline in which NaCl was replaced with Na gluconate ([Cl⁻] = 39

mM). Estimated conductance falls from 33 pS to 29 pS and reversal potential is shifted by +24 mV.

Table 1

Frequency with which the three different types of current were observed in each area and in total. Patches with currents of type 1 and 2 (but not 3) were never seen.

region	anterior acrosomal	equatorial	posterior	total
patches	238	208	8	454
'good' seal	142	102	3	247
activity	38	11	-	49
type I	10	2	-	12
Type 1+2	-	-	-	0
type 1+3	1	1	-	2
type 2+3	-	-	-	0
type 1+2+3	-	7	-	7
Intermittent flickering	27	1	-	28